

Elastic constants of the polycrystalline Bi-Pb-Sr-Ca-Cu-O superconductor

H. M. Ledbetter, S. A. Kim, and R. B. Goldfarb

National Institute of Standards and Technology, Boulder, Colorado 80303

K. Togano

National Research Institute for Metals, Tsukuba, Ibaraki 305, Japan

(Received 13 February 1989)

For polycrystalline $(\text{Bi-Pb})_2\text{Sr}_2\text{Ca}_2\text{Cu}_3\text{O}_{10}$, we report the 5–295-K elastic constants: shear modulus (G), Young modulus (E), bulk modulus (B), and Poisson ratio (ν). Both G and E show nearly normal temperature variation. During cooling, B softens between 215 and 65 K. The Poisson ratio decreases abruptly at 215 K and decreases almost five percent in the 295–5-K region. In its temperature dependence, this compound resembles $\text{YBa}_2\text{Cu}_3\text{O}_7$. However, it shows much lower elastic stiffness. Corrected to the void-free state, we calculate a Debye temperature of 312 K, versus 436 K for $\text{YBa}_2\text{Cu}_3\text{O}_7$. The Poisson ratio, 0.20, agrees well with that of $\text{YBa}_2\text{Cu}_3\text{O}_7$, 0.21. We use Kresin's model to interrelate Debye temperature, critical temperature, and electron-phonon interaction parameter for four classes of copper-oxide superconductors.

The four existing classes of high- T_c metal-oxide superconductors, La-O, Y-O, Bi-O, and Tl-O, have provided the foci for numerous physical-property studies. For Y-O alone, we have noted approximately fifty sound-velocity, elastic-constant studies.¹ Despite many unsettled issues for Y-O, it seems useful to extend such studies to Bi-O, to note the common and uncommon features in the spirit of a single unifying explanation of high- T_c superconductivity in metal oxides.

Relationships of elastic constants to lattice vibrations, electronic structure, and phase transitions are well known. Below, we describe their relationship to various superconductivity parameters, especially the Debye temperature and the electron-phonon-interaction parameter.

We prepared cylindrical specimens 23 mm in diameter and 9 mm thick. We started with the following oxides: Pb_3O_4 , Bi_2O_3 , SrCO_3 , and CuO . We calcined these in air at 800°C for 12 h. Powders were then pressed and sintered in 8% oxygen–92% argon at 835°C for 83 h. Specimens were furnace cooled to 750°C, held for 3 h in flowing oxygen, and furnace cooled in oxygen to room temperature.

To characterize the specimens, we measured electrical resistance by a four-probe method and ac magnetic susceptibility at 100 Hz at rms fields of 0.8, 80, and 800 A/m. We made measurements both parallel and perpendicular to the pressing axis. Figure 1 shows some results. We did x-ray diffraction with $\text{Cu K}\alpha$ radiation on two surfaces: the flat cylinder surface and a perpendicular surface obtained by cutting the specimen. Figure 2 shows the diffraction results.

The electrical resistance begins a sharp decrease near 112 K, and extrapolates to zero at 107 K. The resistance-temperature curve suggests a single-phase transition occurring over a 5-K interval.

The low-field magnetic susceptibility shows a single transition in the real part (χ') and a single peak in the imaginary part (χ''). The transition occurs over a 2-K interval centered near 103 K. The volume susceptibility

fails to extrapolate to -1 because of the approximate demagnetization factor used to process the measured values. The $\chi(T)$ curves showed no dependence on field orientation. In larger fields, two transitions are apparent.² The one at higher temperature is intrinsic, caused by superconducting grains. The lower one arises from coupling between the grains.

The nearly identical x-ray-diffraction patterns suggest absence of significant texture, either surface or volume. (Susceptibility measurements confirmed the absence of texture.) These patterns are dominated by one set of diffraction lines: $(00l)$, with l even. For specimens similar to ours, Koyama, Endo, and Kawai³ reported the unit-cell dimensions: $a = 5.396 \text{ \AA}$ and $c = 37.180 \text{ \AA}$, giving a unit-cell volume of 1082.6 \AA^3 . Comparing these with the unit-cell dimensions reported by Subramanian *et al.*⁴ and by Gao *et al.*⁵ for the 2:2:1:2 Bi-Sr-Ca-Cu-O, we see that the a axes are nearly the same: $5.396/5.406 = 0.998$. The c axes differ by $37.180/30.871 = 1.204$.

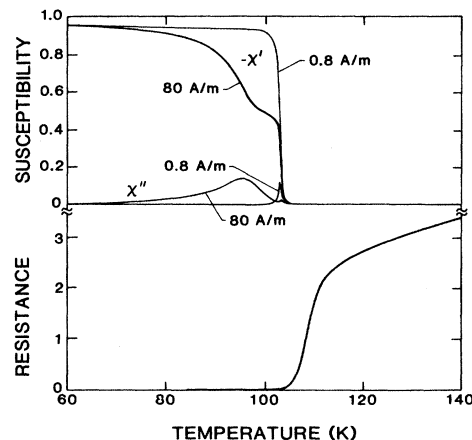


FIG. 1. Temperature variation of electrical resistance and real and imaginary parts of magnetic susceptibility at two fields.

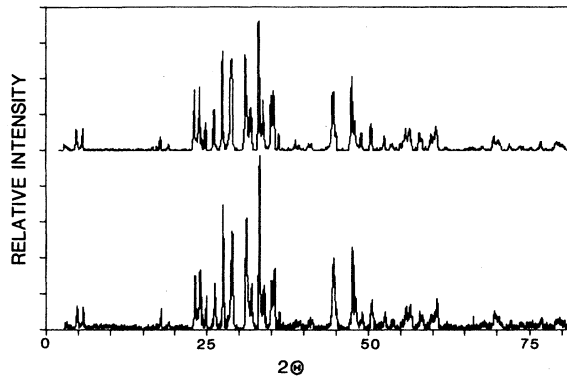


FIG. 2. X-ray-diffraction patterns. Top: from surface of cylindrical pellet. Bottom: from interior surface obtained by diamond-saw cutting.

Thus, we conclude that the present unit cell contains 18 layers, versus 14 in the 2:2:1:2 compound, corresponding probably to intercalation of two Ca-CuO₂ layers. In discussing preparation of the 2:2:2:3 phase, Ikeda *et al.*⁶ gave indexed x-ray-diffraction patterns.

To calculate the theoretical mass density ρ_t we need to know the oxygen stoichiometry. We estimated this by using the homologous-series crystal-chemistry formula given by Santoro *et al.*:⁷ Bi₂Sr₂Ca_{n-1}Cu_nO_{2n+4}. Thus, we assume Bi_{1.84}Pb_{0.34}Sr₂Ca₂Cu₃O₁₀ with a molecular weight of 1061. Taking four molecules per unit cell (identical to the 2:2:1:2 compound) gives $\rho_t = 6.51$ g/cm³. The specimen's macroscopic mass density is $\rho_m = 3.76$. Thus, we estimate that the specimen is 58% dense, or that it contains 42% voids. This agrees with porosity estimated from the 800-A/m χ' curves (not shown). There is an intrinsic plateau at 0.55–0.60 at temperatures of 80–90 K, where the grains are decoupled.²

To determine elastic constants, we measured longitudinal and transverse sound velocities by a MHz-frequency pulse-echo method.

Despite their high void content, the specimens showed excellent ultrasound transmission in the cylinder-axis direction. Figure 3 shows a pulse-echo pattern. Waves propagated in the transverse plane showed much higher attenuation. Table I shows measured sound velocities, effective elastic constants C calculated from $C = \rho v^2$, where ρ denotes mass density and v sound velocity, and elastic constants are corrected to the void-free state by a composite-material model.⁸ For comparison, Table I shows void-free-state elastic constants for a high-quality Y-Ba-Cu-O specimen.⁹ Table I also shows elastic Debye temperatures calculated from v_l , v_t , and ρ by a standard method.⁸ (Here, subscripts l and t denote longitudinal and transverse.) Not shown in Table I, the specimens showed direction-dependent sound velocities, indicating texture, but not revealed by x-ray diffraction. We handled this velocity anisotropy by averaging over three principal directions. We attribute the velocity anisotropy to aligned nonspherical voids between the thin Bi-O plates. For comparison with specific-heat measurements, Table I includes both elastic and calorimetric Debye tempera-

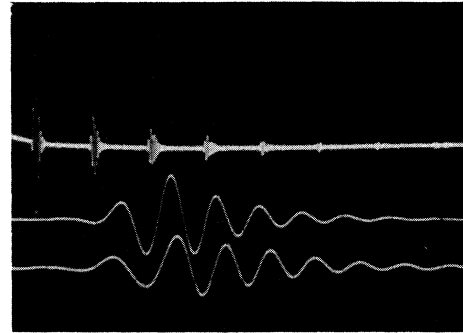


FIG. 3. Composite oscilloscope display of longitudinal-wave pulse-echo pattern for specimen 1. Expanded first and second echoes are shown at bottom. Transit time was measured between the first minimum in these adjacent echoes. Carrier frequency equals 5 MHz and round-trip transit time approximately 6 μ s.

tures: Θ_l^b and Θ_t^b ; the latter appear in a recent review by Fisher, Gordon, and Phillips.¹⁰

Figure 4 shows the temperature dependence of four polycrystalline elastic constants: G =shear modulus, E =Young modulus, B =bulk modulus, ν =Poisson ratio. The voids should affect the absolute elastic constants C , but not the $C(T)$ behavior, as we can see by considering models that correct the elastic constants for void content.⁸ Both G and E show nearly normal behavior. During cooling, B is regular for a while, but it softens between 215 and 65 K. This softening onset shows especially in ν , which shows a surprisingly large change between 295 and 5 K, indicating strong interatomic-bonding changes. The temperature behavior strongly resembles that reported previously for YBa₂Cu₃O₇.^{9,11} The notable difference is that in Y-Ba-Cu-O, the Poisson ratio increases upon cooling below T_c . Like Y-Ba-Cu-O, the present superconductor showed thermal hysteresis, especially in the dilatation-elastic modes. We interpreted this thermal hysteresis

TABLE I. Void-free-state elastic constants of Bi-Pb-Sr-Ca-Cu-O and Y-Ba-Cu-O at $T=295$ K.

	Bi-O Specimen 1 ^a	Bi-O Specimen 2 ^b	Y-O
ρ (g/cm ³)	6.51	6.51	6.35
v_l (cm/ μ s)	0.357	0.374	0.532
v_t (cm/ μ s)	0.231	0.229	0.305
v_m (cm/ μ s)	0.253	0.253	0.339
C_l	82.8	90.8	180.0
G	34.6	34.2	59.0
B	36.6	45.7	100.9
E	79.0	82.0	148.2
ν	0.140	0.198	0.255
Θ_l^b (K)	312	312	437
Θ_t^b (K) ^c	230–290	230–290	450

^aMeasured only along cylinder axis.

^bMeasured along three orthogonal directions and averaged.

^cReference 8.

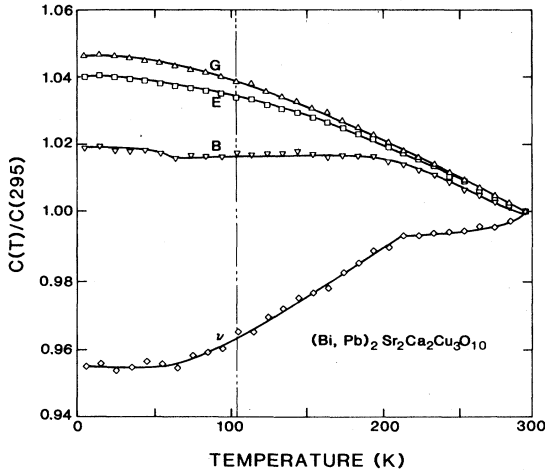


FIG. 4. Temperature variation of four elastic constants: G =shear modulus, E =Young modulus, B =bulk modulus, ν =Poisson ratio. Based on magnetic-susceptibility measurement, $T_c = 103$ K.

as a sluggish phase transition of unknown character, but resembling phase transitions in relaxor ferroelectrics.¹¹ We emphasize that in both materials, within measurement error (about 1 in 1000), no elastic-constant discontinuities occur at T_c .

In Table I, we see a dramatic difference between Bi-Pb-Sr-Ca-Cu-O and Y-Ba-Cu-O. The Bi-O superconductor is elastically much softer (approximately by a factor of 2), in both the dilatational and shear modes. We attribute this softening to weak or nonexistent metal-oxygen bonds along the 18-layer unit cell.

Interestingly, the Poisson ratio, 0.198, falls not far from that of the reported Y-Ba-Cu-O, 0.225, and close to the average ν reported⁹ for six specimens, 0.212. More than any other elastic constant, the Poisson ratio relates to type of interatomic bonding.¹² Thus, despite large elastic-stiffness differences, similar Poisson ratios suggest similar interatomic bonding.

The Debye temperature Θ_D shown in Table I may be inaccurate because of the large correction for 42% voids. In this correction, we assumed spherical voids. Any other void shape would give a higher void-free state Θ_D . We estimate the Θ_D error as 20% or less; thus Θ_D lies probably in the range $250 < \Theta_D < 374$ K. Fisher, Gordon, and Phillips,¹⁰ for four different Bi-O stoichiometries, reported specific-heat Debye temperatures of 230–290 K. Thus, we find reasonable agreement between the specific-heat and elastic Debye temperatures.

The Debye temperature figures prominently in most existing superconductivity models. The original BCS model¹³ gives for the transition temperature

$$T_c = 1.14\Theta_D \exp(-1/\lambda). \quad (1)$$

Here, λ denotes the electron-phonon interaction parameter, which varies as¹³

$$\lambda \sim \Theta_D^{-2}. \quad (2)$$

McMillan's¹⁴ stronger coupling model retains Θ_D :

$$T_c \frac{\Theta_D}{1.45} \exp\left[-\frac{1.04(1+\lambda)}{\lambda - \mu^*(1+0.62\lambda)}\right]. \quad (3)$$

Here, μ^* denotes the electron-phonon Coulomb-repulsion pseudopotential, which also depends on Θ_D .¹⁴ Both Eqs. (1) and (3) predict a maximum T_c corresponding to $\lambda = 2$, thus an optimum Θ_D . Recent results by Kresin¹⁵ based on the Eliashberg equation and valid for all λ , predict no maximum in $T_c(\Theta_D)$. Kresin derived the following relationship:

$$T_c = 0.254\Theta_D(e^{2/\lambda} - 1)^{-1/2}. \quad (4)$$

Figure 5 shows T_c - Θ_D graphs of this equation for η' [Eq. (5)] chosen to pass through points representing the four principal oxide superconductors: La-O, Y-O, Bi-O, and Tl-O. Kresin's equation predicts that, for the same η (the McMillan-Hopfield parameter), a lower Θ_D (softer modes) yields a higher T_c . But, we see discouragement in the small slope $dT_c/d\Theta_D$ and in the impracticality of reducing Θ_D much lower, except perhaps in localized modes. To raise T_c dramatically, we need to find materials with higher η' , where

$$\lambda = \eta'\Theta_D^{-2} = \eta/M, \quad (5)$$

where

$$\eta = \langle I^2 \rangle N(0), \quad (6)$$

where M , $\langle I^2 \rangle$, and $N(0)$ take their usual meanings:¹⁵ M denotes oscillator mass, $N(0)$ the electron-band density of states at the Fermi surface, and $\langle I^2 \rangle$ an average of the electron-phonon matrix element over the Fermi surface. In Kresin's model, T_c/Θ_D can assume large values ($T_c/\Theta_D = 0.5$ for $\lambda \approx 10$).

Using Kresin's model and the measured T_c 's and Θ_D 's, we obtain the following electron-phonon parameters, λ : 0.92 (La-O), 2.32 (Y-O), 4.52 (Bi-O), and 7.96 (Tl-O). The first two seem reasonable. Using a strong-coupling

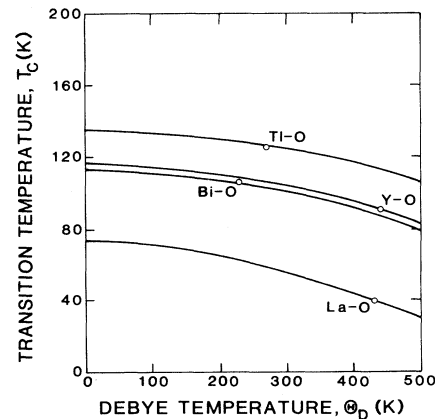


FIG. 5. Transition temperature vs Debye temperature. Curves from Kresin model for constant McMillan-Hopfield parameter η . Points represent four classes of high- T_c metal-oxide superconductors: La-O, Y-O, Bi-O, and Tl-O.

version of Usadel's dirty-limit theory, Rammer¹⁶ calculated $\lambda \approx 2$ for La-O, and $\lambda \approx 5$ for Y-O. It is interesting that our results predict a lower λ for Y-O than for Bi-O, and that soft phonon modes^{17,18} are not required to achieve a high enough λ .

In summary, we find that Bi-Pb-Sr-Ca-Cu-O shows almost the same temperature behavior as Y-Ba-Cu-O. But it is much softer elastically, showing an elastic Debye temperature of 312 K versus 437 K for Y-Ba-Cu-O. Like Y-

Ba-Cu-O, it shows hysteresis, bulk-modulus softening during cooling, and a large Poisson-ratio change. Perhaps reflecting similar interatomic bonding, the Poisson ratios show similar values.

We acknowledge contributions by M. Austin (x-ray diffraction), M. Lei (Kresin-model calculations), R. Loughran (ac susceptibility), and E. Yanagisawa of Asahi Glass (material preparation).

¹List, omitted for brevity, available from authors.

²R. B. Goldfarb, A. F. Clark, A. I. Braginski, and A. J. Panson, *Cryogenics* **27**, 475 (1987).

³S. Koyama, U. Endo, and T. Kawai, *Jpn. J. Appl. Phys.* **2**, L1861 (1988).

⁴M. A. Subramanian, C. C. Torandi, J. C. Calabrese, J. Gopalakrishnan, K. J. Morrissey, T. R. Askew, R. B. Flippen, U. Chowdry, and A. W. Sleight, *Science* **239**, 1015 (1988).

⁵Y. Gao, P. Lee, P. Coppens, M. A. Subramanian, and A. W. Sleight, *Science* **241**, 954 (1988).

⁶Y. Ikeda, M. Takano, Z. Hiroi, K. Oda, H. Kitaguchi, J. Takada, Y. Miura, Y. Takeda, O. Yamamoto, and H. Mazaki, *Jpn. J. Appl. Phys.* **27**, L1067 (1988).

⁷A. Santoro, F. Beech, M. Marezio, and R. J. Cava, *Physica C* **156**, 693 (1988).

⁸H. M. Ledbetter, M. W. Austin, S. A. Kim, and Ming Lei, *J. Mater. Res.* **2**, 786 (1987).

⁹H. M. Ledbetter, in *Shape Memory Metals*, edited by K. Otsuka and K. Shimizu, Proceedings of the Materials Research Society International Meeting on Advanced Materials, Vol. 9 (Materials Research Society, Pittsburgh, PA, in press).

¹⁰R. A. Fisher, J. E. Gordon, and N. E. Phillips, *J. Supercond.* (to be published).

¹¹H. M. Ledbetter and S. A. Kim, *Phys. Rev. B* **38**, 11857 (1988).

¹²W. Köster and H. Franz, *Metallogr. Rev.* **6**, 1 (1961).

¹³J. Bardeen, L. N. Cooper, and J. R. Schrieffer, *Phys. Rev.* **108**, 1175 (1957).

¹⁴W. McMillan, *Phys. Rev.* **167**, 331 (1968).

¹⁵V. Z. Kresin, *Phys. Lett. A* **122**, 434 (1987).

¹⁶J. Rammer, *Phys. Rev. B* **36**, 5665 (1987).

¹⁷W. Weber, *Phys. Rev. Lett.* **58**, 1371 (1987).

¹⁸W. E. Pickett, H. Krakauer, D. A. Papaconstantopolous, and L. L. Boyer, *Phys. Rev. B* **35**, 7252 (1987).

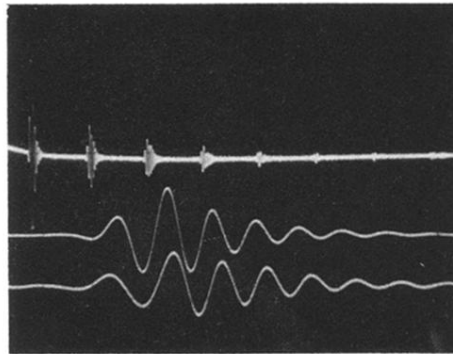


FIG. 3. Composite oscilloscope display of longitudinal-wave pulse-echo pattern for specimen 1. Expanded first and second echoes are shown at bottom. Transit time was measured between the first minimum in these adjacent echoes. Carrier frequency equals 5 MHz and round-trip transit time approximately $6 \mu\text{s}$.